

# Rhodium(III), Palladium(II), and Platinum(II) Complexes with 2-(2-Hydroxybenzoyl)-*N*-Methylhydrazinecarbothioamide: Syntheses, Structures, and Spectral Characteristics

S. I. Orysyk<sup>a,\*</sup>, V. V. Bon<sup>a</sup>, O. A. Zholob<sup>a</sup>, V. I. Pekhnyo<sup>a</sup>, V. V. Orysyk<sup>b</sup>,  
Yu. L. Zborovskii<sup>b</sup>, and M. V. Vovk<sup>b</sup>

<sup>a</sup> Vernadsky Institute of General and Inorganic Chemistry, National Academy of Sciences of Ukraine,  
pr. akademika Palladina 32/34, Kiev, Ukraine

<sup>b</sup> Institute of Organic Chemistry, National Academy of Sciences of Ukraine, ul. Murmanskaya 5, Kiev, Ukraine

\*e-mail: oryisyk@ionc.kiev.ua

Received August 4, 2013

**Abstract**—The syntheses and spectral (IR, UV-VIS, XPS, and <sup>1</sup>H and <sup>13</sup>C NMR) characteristics of the rhodium(III), palladium(II), and platinum(II) complexes with 2-(2-hydroxybenzoyl)-*N*-methylhydrazinecarbothioamide (HBMHCTA) are described. The coordination of HBMHCTA to the central metal ion and its intraligand rearrangement in the complex formation of rhodium(III) ions are studied. The structure of the mixed-ligand complex [Pd(H<sub>2</sub>L)PPh<sub>3</sub>] is determined by X-ray diffraction analysis.

DOI: 10.1134/S1070328414030063

## INTRODUCTION

Thiosemicarbazides are of special interest as complexing agents for transition and platinum group metals. The introduction of additional functional groups into the structures of thiosemicarbazides increases the number of possible coordination modes. Thiosemicarbazides are prototropic ligand systems and, hence, they are coordinated as certain tautomeric forms, depending on the nature of substituents and synthesis conditions, upon the interaction with metal ions [1–5]. In particular, 2-(2-hydroxybenzoyl)-*N*-methylhydrazinecarbothioamide (HBMHCTA, H<sub>4</sub>L) containing a series of nucleophilic functional groups (OH, C=O, NH, C=S) and capable of participating in the formation of donor–acceptor bonds with metal ions is a promising complexing agent characterized by the amidoimidol and/or thione-thiol tautomerism. The latter provides the coordination to the central metal atom in different tautomeric forms. Depending on the synthesis conditions and metal nature, the tautomers can form coordination compounds of various compositions, structures, and properties.

The thiosemicarbazone complexes with Pd<sup>2+</sup> ions were shown [6] to be efficient catalysts in the Buchwald–Hartwig amination and in carbon–carbon bonding [7–10]. In addition, the complexes of thiosemicarbazide derivatives with palladium and platinum have high biological activities (anticancer, antimalarial, antiviral, anti-inflammatory, fungicidal, immunostimulating, and cardiotoxic) and, hence, can be considered as potent drugs [11–15]. Therefore, the investigation of the complex formation of polydentate

HBMHCTA with Rh<sup>3+</sup>, Pd<sup>2+</sup>, and Pt<sup>2+</sup> ions, which differ in electronic structure and coordination capacity, is an important stage in the development of the targeted synthesis of practically interesting complexes with certain composition and structure.

## EXPERIMENTAL

Commercial RhCl<sub>3</sub> · 4H<sub>2</sub>O (39.51% Rh), PdCl<sub>2</sub> (59.0% Pd), K<sub>2</sub>[PtCl<sub>4</sub>] (43.6% Pt), and PdCl<sub>2</sub>(PPh<sub>3</sub>)<sub>2</sub> (24.0% Pd) were used as the starting metal salts for the syntheses of the complexes.

**Synthesis of HBMHCTA (H<sub>4</sub>L).** Methyl isothiocyanate (7.67 g, 0.105 mol) was added to a suspension of salicylic acid hydrazide (15.21 g, 0.1 mol) in ethanol (70 mL). The reaction mixture was refluxed in a water bath for 1 h. After cooling, the crystalline product H<sub>4</sub>L was filtered off, washed with ethanol cooled to 0°C and diethyl ether, and recrystallized from ethanol. The yield was 18.25 g (81%), mp = 214–215°C.

For C<sub>9</sub>H<sub>11</sub>N<sub>3</sub>O<sub>2</sub>S

anal. calcd., %: C, 47.99; H, 4.90; N, 18.66; S, 14.22.

Found, %: C, 47.89; H, 4.75; N, 18.93; S, 13.97.

<sup>1</sup>H NMR, δ, ppm: 2.88 d (3H, C<sup>9</sup>H<sub>3</sub>, *J* = 4.5 Hz), 6.90–6.96 m (2H, C<sup>5,7</sup>H<sub>Ar</sub>), 7.45 t (1H, C<sup>6</sup>H<sub>Ar</sub>, *J* = 8.4 Hz), 7.87 d (1H, C<sup>8</sup>H<sub>Ar</sub>, *J* = 7.2 Hz), 8.13 s (1H, N<sup>c</sup>H), 9.45 s (1H, N<sup>a</sup>H), 10.55 s (1H, N<sup>b</sup>H), 11.95 s (1H, OH). <sup>13</sup>C NMR, δ, ppm: 31.40 C<sup>9</sup>, 115.14 C<sup>2</sup>, 117.52 C<sup>6</sup>, 119.47 C<sup>5</sup>, 129.10 C<sup>7</sup>, 134.82 C<sup>3</sup>, 159.67 C<sup>3</sup>, 169.02 C<sup>1</sup>, 182.42 C<sup>8</sup>.

**Synthesis of [Rh(H<sub>3</sub>L)<sub>2</sub>]Cl (I).** RhCl<sub>3</sub> · 4H<sub>2</sub>O (0.143 g, 0.5 mmol) was dissolved in ethanol (25 mL) acidified with 4 N HCl (0.2 mL) at 35–40°C. A solution of HBMHCTA (0.225 g, 1 mmol) in ethanol (10 mL) was added with stirring to the obtained solution for 3 min. The reaction mixture was refluxed for 30 min. The formed brown precipitate was filtered off, washed with ethanol and diethyl ether, and dried in a drying box above CaCl<sub>2</sub>. The yield was 0.158 g (54%), decomposition temperature ≥270°C.

For C<sub>18</sub>H<sub>20</sub>N<sub>6</sub>O<sub>4</sub>S<sub>2</sub>ClRh

anal. calcd., %: C, 36.84; H, 3.43; N, 14.32; S, 10.93; Cl, 6.04; Rh, 17.53.

Found, %: C, 36.59; H, 3.55; N, 13.99; S, 11.08; Cl, 5.73; Rh, 17.23.

<sup>1</sup>H NMR, δ, ppm: 2.96 d (3H, C<sup>9</sup>H<sub>3</sub>, *J* = 4.5 Hz), 6.60–6.95 m (2H, C<sup>5,7</sup>H<sub>Ar</sub>), 7.48 t (1H, C<sup>6</sup>H<sub>Ar</sub>, *J* = 8.2 Hz), 7.96 d (1H, C<sup>8</sup>H<sub>Ar</sub>, *J* = 7.2 Hz), 8.76 s (1H, N<sup>c</sup>H), 10.89 s (1H, N<sup>a</sup>H), 11.39 s (1H, N<sup>b</sup>H).

**Synthesis of [Rh(KL')<sub>3</sub>] (II).** RhCl<sub>3</sub> · 4H<sub>2</sub>O (0.143 g, 0.5 mmol) was dissolved in ethanol (25 mL) at 35–40°C. A solution of HBMHCTA (0.225 g, 1 mmol) in a 0.1 N solution of KOH (30 mL) was added with stirring to the obtained solution for 3 min. The reaction mixture was refluxed for 60 min, and the formed light brown precipitate was filtered off, washed with ethanol and diethyl ether, and dried in a drying box above CaCl<sub>2</sub>. The yield was 0.192 g (46%), decomposition temperature ≥235°C.

For C<sub>27</sub>H<sub>21</sub>N<sub>9</sub>O<sub>3</sub>S<sub>3</sub>K<sub>3</sub>Rh

anal. calcd., C, 38.79; H, 2.53; N, 15.08; S, 11.51; Rh, 12.31. %:

Found, %: C, 39.02; H, 2.65; N, 14.92; S, 11.67; Rh, 12.67.

<sup>1</sup>H NMR, δ, ppm: 2.88 m (3H, C<sup>9</sup>H<sub>3</sub>), 6.67 m (1H, C<sup>5</sup>H<sub>Ar</sub>), 7.04 m (1H, C<sup>7</sup>H<sub>Ar</sub>), 7.97–8.07 m (2H, C<sup>6,8</sup>H<sub>Ar</sub>).

**Synthesis of [Pd(H<sub>2</sub>L)(H<sub>4</sub>L)] (III).** PdCl<sub>2</sub> (0.097 g, 0.55 mmol) was dissolved in a mixture of ethanol (25 mL) and 4 N HCl (0.2 mL) at 35–40°C. A solution of HBMHCTA (0.248 g, 1.1 mmol) in ethanol (10 mL) was added with stirring to the obtained solution for 3 min. The reaction mixture was refluxed for 15 min, and the formed amorphous flesh-colored precipitate was filtered off, washed with ethanol and diethyl ether, and dried in a drying box above CaCl<sub>2</sub>. The yield was 0.235 g (77%), decomposition temperature ≥255°C.

For C<sub>18</sub>H<sub>20</sub>N<sub>6</sub>O<sub>4</sub>S<sub>2</sub>Pd

anal. calcd., %: N, 15.14; S, 11.55; Pd, 19.18.

Found, %: N, 15.45; S, 11.32; Pd, 18.87.

<sup>1</sup>H NMR, δ, ppm: 2.89/2.94 dd (6H, C<sup>9</sup>H<sub>3</sub>, C<sup>9'</sup>H<sub>3</sub>, *J* = 4.5, *J* = 14.7 Hz), 6.58 m (2H, C<sup>5,7</sup>H<sub>Ar</sub>), 6.98 m (3H,

C<sup>5',7',6'</sup>H<sub>Ar</sub>), 7.47 m (1H, C<sup>6</sup>H<sub>Ar</sub>), 7.88–7.98 m (3H, C<sup>8,8'</sup>H<sub>Ar</sub> + 1H, NH), 8.87 s (1H, N<sup>c</sup>H), 10.79 s (1H, N<sup>a</sup>H), 11.60 s (1H, N<sup>b</sup>H), 12.53 s (1H, OH). <sup>13</sup>C NMR, δ, ppm: 30.6/31.8 C<sup>9</sup>, 115.5/118.1 C<sup>2</sup>, 116.0/117.6 C<sup>Ar</sup>, 119.5/120.4 C<sup>Ar</sup>, 129.42/131.2 C<sup>Ar</sup>, 131.3/134.8 C<sup>Ar</sup>, 159.2/158.1 C<sup>3</sup>, 167.8/162.9 C<sup>1</sup>, 178.2/168.4 C<sup>8</sup>.

**Synthesis of [Pt(H<sub>2</sub>L)(H<sub>4</sub>L)] (IV).** K<sub>2</sub>[PtCl<sub>4</sub>] (0.083 g, 0.2 mmol) was dissolved in water (10 mL) at 35–40°C, and the volume was brought with ethanol to 25 mL. A solution of HBMHCTA (0.095 g, 0.42 mmol) was added with stirring to the obtained solution for 3 min. The reaction mixture was refluxed for 15 min. The formed light green amorphous precipitate was filtered off, washed with ethanol and diethyl ether, and dried in a drying box above CaCl<sub>2</sub>. The yield was 0.080 g (62%), decomposition temperature ≥265°C.

For C<sub>18</sub>H<sub>20</sub>N<sub>6</sub>O<sub>4</sub>S<sub>2</sub>Pt

anal. calcd., %: N, 13.06; S, 9.95; Pt, 30.31.

Found, %: N, 12.76; S, 10.21; Pt, 29.89.

<sup>1</sup>H NMR, δ, ppm: 2.90/2.96 dd (6H, C<sup>9</sup>H<sub>3</sub>, C<sup>9'</sup>H<sub>3</sub>, *J* = 4.5, *J* = 14.7 Hz), 6.65 m (2H, C<sup>5,7</sup>H<sub>Ar</sub>), 6.98 m (3H, C<sup>5',7',6'</sup>H<sub>Ar</sub>), 7.08–7.46 m (1H, C<sup>6</sup>H<sub>Ar</sub>), 7.85–8.07 m (3H, (3H, C<sup>8,8'</sup>H<sub>Ar</sub> + 1H, N<sup>c</sup>H), 8.88 s (1H, N<sup>c</sup>H), 10.78 s (1H, N<sup>a</sup>H), 11.60 s (1H, N<sup>a</sup>H), 11.87 s (1H, N<sup>b</sup>H), 12.11 s (1H, OH). <sup>13</sup>C NMR, δ, ppm: 30.7/31.4 C<sup>9</sup>, 115.0/115.8 C<sup>2</sup>, 117.2/119.0 C<sup>Ar</sup>, 117.4/120.6 C<sup>Ar</sup>, 129.0/131.5 C<sup>Ar</sup>, 130.7/134.3 C<sup>Ar</sup>, 159.0/155.6 C<sup>3</sup>, 167.6/162.5 C<sup>1</sup>, 176.8/168.0 C<sup>8</sup>.

**Synthesis of [Pd(H<sub>2</sub>L)(PPh<sub>3</sub>)] (V).** A solution of HBMHCTA (0.022 g, 0.098 mmol) in ethanol (20 mL) was carefully added to a solution of PdCl<sub>2</sub>(PPh<sub>3</sub>)<sub>2</sub> (0.044 g, 0.062 mmol) in chloroform (20 mL) in such a way that mixing of the chloroform and ethanol phases would be prevented. The mixture was kept in a closed light-proof vessel for 3 weeks. The reaction product was formed as yellow plate-like single crystals. The yield was 0.025 g (67%), decomposition temperature ≥301°C.

For C<sub>27</sub>H<sub>24</sub>N<sub>3</sub>O<sub>2</sub>PSPd

anal. calcd., %: N, 7.09; S, 5.41; Pd, 17.97.

Found, %: N, 6.97; S, 5.28; Pd, 17.78.

<sup>1</sup>H NMR, δ, ppm: 2.86 d (3H, C<sup>9</sup>H<sub>3</sub>, *J* = 4.2 Hz), 6.90–6.97 m (3H, C<sup>5,7</sup>H<sub>Ar</sub> and PPh<sub>3</sub>), 7.25 m (2H, PPh<sub>3</sub>), 7.42–7.65 m (13H, PPh<sub>3</sub>, C<sup>6</sup>H<sub>Ar</sub>), 7.88 d (1H, C<sup>8</sup>H<sub>Ar</sub>, *J* = 8.1 Hz), 8.14 br.m (1H, N<sup>c</sup>H), 9.49 s (1H, N<sup>a</sup>H).

**Table 1.** Crystallographic data and the main refinement parameters for complex **V**

Parameter	Value
Crystal size, mm	0.35 × 0.15 × 0.05
Crystal system	Triclinic
Space group	$P\bar{1}$
<i>a</i> , Å	9.9053(2)
<i>b</i> , Å	12.0524(3)
<i>c</i> , Å	12.2174(3)
$\alpha$ , deg	64.8300(10)
$\beta$ , deg	81.1300(10)
$\gamma$ , deg	67.4410(10)
<i>V</i> , Å <sup>3</sup>	1218.98(5)
<i>Z</i>	2
$\rho_{\text{calcd}}$ , g/cm <sup>-3</sup>	1.613
$\mu$ , mm <sup>-1</sup>	0.944
<i>F</i> (000)	600
$\theta$ range, deg	1.84–30.57
Index range	$-14 \leq h \leq 14,$ $-17 \leq k \leq 17, -17 \leq l \leq 17$
Number of all reflections/independent ( <i>R</i> <sub>int</sub> )	34138/7411 (0.0476)
Reflections with <i>I</i> > 4 $\sigma$ ( <i>I</i> )	6216
Number of refined parameters	325
Goodness-of-fit ( <i>F</i> <sup>2</sup> )	1.047
<i>R</i> <sub>1</sub> , <i>wR</i> <sub>2</sub> ( <i>I</i> ≥ 4 $\sigma$ ( <i>I</i> ))	0.0323, 0.0685
<i>R</i> <sub>1</sub> , <i>wR</i> <sub>2</sub> (all reflections)	0.0432, 0.0738
$\Delta\rho_{\text{max}}/\Delta\rho_{\text{min}}$ , e Å <sup>-3</sup>	0.640/−0.696

The elemental compositions of the complexes were determined by electron-probe X-ray microanalysis (VRA-30 spectrometer, 45 kV, W anode, membrane diameter 7 mm, samples in KBr pellets). The relative intensity of the Pd $K_{\alpha}$  lines was 04085 (03660, 0.0676), and the probable uncertainty for the background was  $\leq 0.0100$ . The relative intensity of the Br $K_{\alpha}$  line was  $1.647 \pm 0.005$ , and the probable uncertainty for the background was  $\pm 0.0015$ . The program for the calculation of analytical line intensities by the method of relationship equations to fundamental parameters was applied to determine the quantitative characteristics. Elemental analyses were carried out in parallel using the classical methods: nitrogen was determined by the Dumas method, chlorine and sulfur were determined using the volumetric method after the combustion of a weighed sample in oxygen, and carbon and hydrogen were determined according to Pregle's method.

The UV-VIS spectra of the complexes were recorded on a Specord M-40 spectrophotometer (50000–11000 cm<sup>-1</sup>) in quartz cells with *l* = 0.1 cm. IR spectra were detected on a Specord M80 spectrophotometer (KBr pellets). <sup>1</sup>H and <sup>13</sup>C NMR spectra were measured on Varian VXR (300 MHz) and Bruker Avance DRX-500 (125.75 MHz) spectrometers in DMSO-*d*<sub>6</sub> with tetramethylsilane.

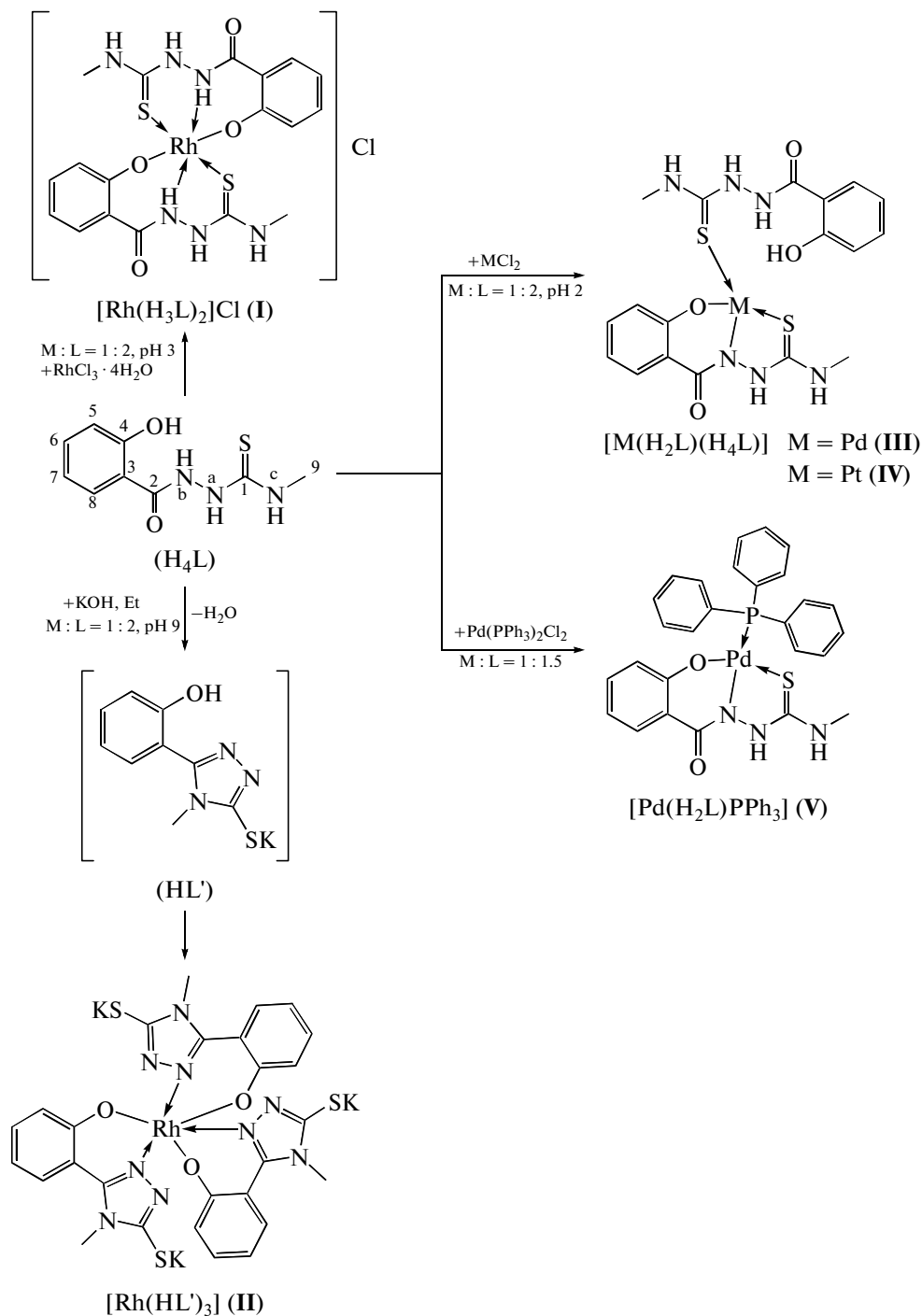
X-ray photoelectron spectra (XPS) were obtained on an ES-2402 spectrometer with PHOIBOS-100-SPECS energy analyzer (Mg $K_{\alpha}$  1253.6 eV, 200 W, *P* =  $2 \times 10^{-7}$  Pa). The spectrometer was equipped with an IQE-11/35 ion gun and FG-15/40 slow electron gun for the compensation of surface charging effects. The spectra were calibrated by the C1s line (*E*<sub>p</sub> = 285.0 eV). The Pd3*d* spectra were decomposed to pairs of components with the parameters *I*<sub>3/2</sub>/*I*<sub>5/2</sub> = 0.66,  $\Delta E_p$  (3*d*<sub>3/2</sub>–3*d*<sub>5/2</sub>) = 4.6 and 5.3 eV, respectively. The full width at the half height (FWHH) of the line was 1.2 and 1.0 eV, respectively. For the S2*p* level, *I*<sub>1/2</sub>/*I*<sub>3/2</sub> = 0.5, FWHH = 1.2 eV, and  $\Delta E_p$  (2*p*<sub>1/2</sub>–2*p*<sub>3/2</sub>) = 1.0 eV. The N1s spectra were decomposed to components with FWHH = 1.3 eV. The composition was performed using the Gauss–Newton method. The surface areas of the components were determined after background subtraction according to the Shirley method.

The electrophoregrams of solutions of the complexes were obtained on chromatography paper strips at a voltage of 280–300 V for 25–30 min. A 0.8 N solution of lithium chloride (ethanol–water) served as a supporting electrolyte [16].

**X-ray diffraction analysis.** Unit cell parameters and a three-dimensional array of reflection intensities for a single crystal of complex **V** were obtained on a Bruker SMART APEX II diffractometer (Mo $K_{\alpha}$  radiation,  $\lambda$  = 0.71073 Å, graphite monochromator) at 173(1) K. The structure was solved by a direct method and refined for *F*<sup>2</sup> by the full-matrix least-squares method using the SHELXTL program package [17]. The hydrogen atoms bound to the nitrogen atoms were revealed from the difference electron density synthesis and refined without restraints imposed by geometric and thermal parameters. The hydrogen atoms bound to the C atoms were specified in geometrically idealized positions according to the hybridization of the accompanying carbon atom and refined using the riding model with *U*<sub>iso</sub> = 1.5*U*<sub>eq</sub> in the case of the CH<sub>3</sub> group and *U*<sub>iso</sub> = 1.2*U*<sub>eq</sub> in all other cases. The main X-ray diffraction data are given in Table 1. The full set of data for compound **V** was deposited with the Cambridge Crystallographic Data Centre (no. 800401; deposit@ccdc.cam.ac.uk or http://www.ccdc.cam.ac.uk).

## RESULTS AND DISCUSSION

The complexes were synthesized by the reactions of the components on heating in an ethanol solution according to the scheme



Scheme.

The reaction of HBMHCTA with rhodium trichloride at pH 3 and the reactant ratio  $M:L = 1:2$  afforded complex I with the tridentate coordination mode of the ligand and formation of five- and six-membered chelate metalocycles through the sulfur, nitrogen, and oxygen atoms of the  $C=S$  and  $NH$  functional groups and deprotonated  $OH$  group. Under

similar conditions,  $K_2[PtCl_4]$  and  $PdCl_2$  form complexes III and IV containing two ligand molecules, one of which is coordinated to the metal ion by the tridentate-chelating mode, and another ligand is coordinated by the monodentate mode only by the sulfur atom of the carbothioamide group as described earlier [1, 18]. The competitive functional  $C=O$  group is not

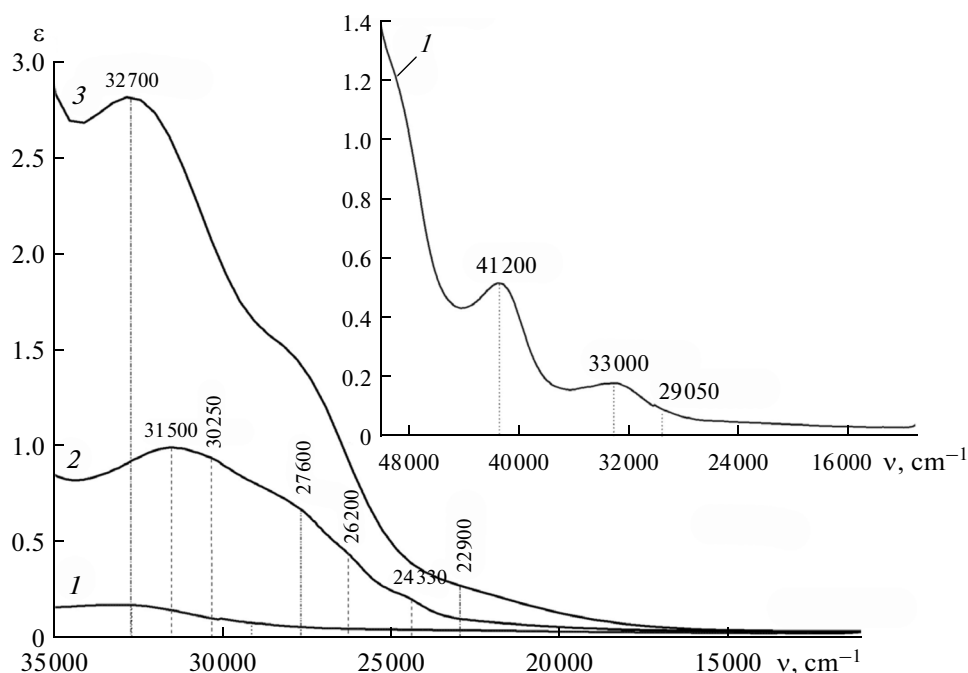


Fig. 1. UV-VIS spectra of HBMHCTA and the rhodium complexes in  $C_2H_5OH$ : (1) HBMHCTA, (2) I, and (3) II.

involved in the donor–acceptor interaction with the metal ions because of a sterically more favorable arrangement of other functional groups.

The reaction of HBMHCTA with  $RhCl_3 \cdot 4H_2O$  at pH 9 results in the formation of complex II including three molecules of 2-(5-mercapto-4-methyl-4*H*-[1,2,4]triazol-3-yl)phenol S-potassium salt (HL) formed due to the cyclization of HBMHCTA in an alkaline medium, being consistent with published data [19].

The reaction of HBMHCTA with  $PdCl_2(PPh_3)_2$  in chloroform gives mixed-ligand complex V in which the HBMHCTA molecule, as in compounds III and IV, is coordinated to the palladium atom by the tridentate-cyclic mode through the sulfur atom of the C=S group and through nitrogen and oxygen of the deprotonated NH and OH groups, respectively.

Complex I containing the chloride anion in the external sphere can dissociate in an aqueous solution to form the complex cation, which was established by electrophoresis on paper [16]. The movement of the colored spot towards the cathode confirms a positive charge of the complex ion.

The UV-VIS, IR, XPS, and  $^1H$  and  $^{13}C$  NMR spectra of  $H_4L$  and complexes I–V were studied in order to establish the coordination mode of the ligand and the shape of the coordination node.

The high-frequency region of the UV-VIS spectrum of HBMHCTA contains an intense band of  $\pi \rightarrow \pi^*$  transitions in the benzene ring at  $41200\text{ cm}^{-1}$  (Fig. 1). In addition, the broadened absorption band with a maximum at  $33000\text{ cm}^{-1}$  characterizes the  $\pi \rightarrow$

$\pi^*$  transition of the C=O carbonyl group. The predominant effect of this transition compensates the effect of the  $n \rightarrow \pi^*$  transition of the C=S group at  $29050\text{ cm}^{-1}$ . As a result, the  $\pi \rightarrow \pi^*$  transition can be identified only after the decomposition of the spectrum to Gaussian components.

An analysis of the UV-VIS spectra of complex I showed that the low-frequency spectral range contains shoulder-like absorption bands at  $24330$ ,  $26200$ , and  $27600\text{ cm}^{-1}$  characterizing the  $^1A_{1g} \rightarrow ^1T_{1g}$ ,  $^1A_{1g} \rightarrow ^1T_{2g}$  electron transitions [20] in the  $Rh^{3+}$  ion, respectively, and the ligand-to-metal charge-transfer (LMCT) transitions  $Rh \rightarrow S$ . Other absorption bands at  $30250$  and  $31500\text{ cm}^{-1}$  are caused by the charge-transfer transition  $N \rightarrow Rh$  and intraligand  $n \rightarrow \pi^*$  transitions of the C=O group [21–23]. This character of the spectrum of the complex is caused by its octahedral structure and the appearance of the corresponding chromophores [Rh–S], [Rh–N], and [Rh–O] due to the coordination of the ligand to metal.

The absorption band of the  $d-d$  transition in the  $Rh^{3+}$  ion of complex II appears at  $22900\text{ cm}^{-1}$ . The next two absorption bands are due to the intraligand LMCTT and the  $n \rightarrow \pi^*$  transition of the C=N groups of the triazole fragment formed by the intraligand rearrangement and the appearance of the corresponding chromophore [Rh–N] at  $32700\text{ cm}^{-1}$  [22].

An analysis of the UV-VIS spectra of complexes III and V in a dimethylformamide solution shows that the absorption in the frequency range from  $26150$  to  $26400\text{ cm}^{-1}$  is caused by the spin-allowed  $d-d$  transitions between the ground energy level  $^1A_{1g}$  and  $^1A_{2g}$ ,

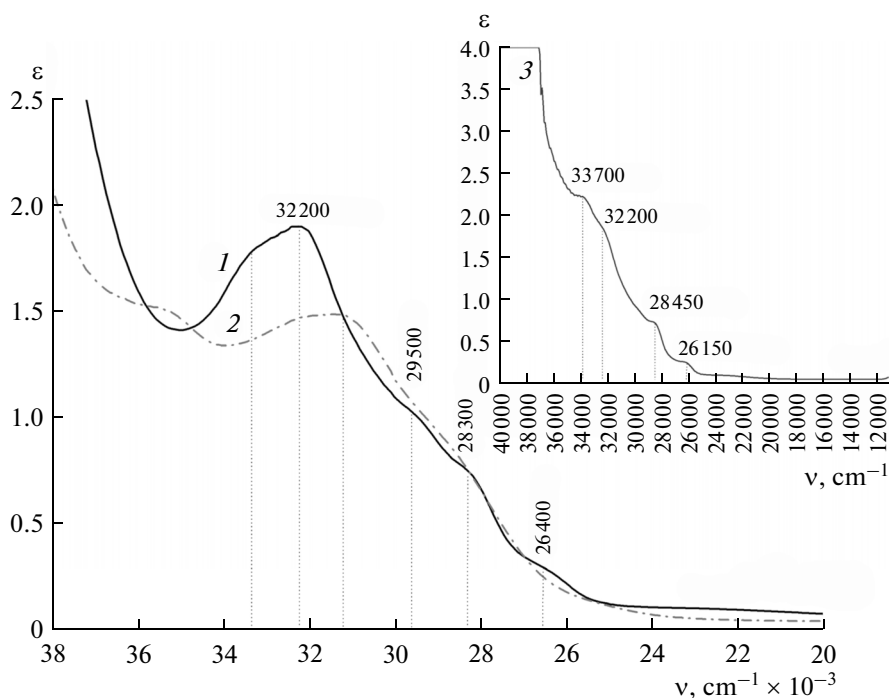


Fig. 2. UV-VIS spectra of complexes **III–V** in dimethylformamide: (1) **III**, (2) **IV**, and (3) **V**.

which are characteristic of the planar-square shape of the coordination node of Pd(II) [23] (Fig. 2). No  $d-d$  spin-allowed transition for the  $Pt^{2+}$  ion is observed in the spectrum of complex **IV**, because this transition is overlapped with the  $n \rightarrow \pi^*$  transition of the C=S chromophore group of the ligand at  $28300\text{ cm}^{-1}$  [23–26].

In the high-frequency spectral range, the intense absorption bands at  $28300\text{--}29500$ ,  $32200\text{--}33700\text{ cm}^{-1}$  (**III**, **V**) and  $31200\text{--}32200$ ,  $35500\text{ cm}^{-1}$  (**IV**) are due to the charge transfer in the intraligand  $n \rightarrow \pi^*$  transitions of the C=S/C=O groups and the  $\pi \rightarrow \pi^*$  transitions of the benzene ring [1, 2, 18, 20, 27–29] and LMCTT [1, 2, 18, 28, 29]. The presented frequency range exhibits the absorption band of the LMCTT  $S \rightarrow M$  at  $28300\text{ cm}^{-1}$  (**III**, **IV**) and  $28450\text{ cm}^{-1}$  (**V**), which is related to the participation of the C=S group of the ligand in coordination to the central metal ion. The positions of the absorption bands at  $33000\text{--}35000$  and  $26400\text{ cm}^{-1}$  indicate the formation of a chromophore consisting of the Pd, S, O, and N atoms.

Thus, the experimental UV-VIS spectral data show that HBMHCTA in complexes **I–V** is coordinated to the central metal ion simultaneously through the donating atoms of nitrogen ( $NH_{amide}$ ), sulfur (C=S), and oxygen of the deprotonated OH group to form the octahedral (for the rhodium complexes) and square (for the palladium and platinum complexes) coordination modes.

The IR spectrum of HBMHCTA exhibits the  $\nu(C=O)$  stretching vibration band at  $1640\text{ cm}^{-1}$  and the broad band at  $3200\text{ cm}^{-1}$  caused by  $\nu(N-H)$  stretching vibrations [1, 26]. The vibrations of the hydroxyl group joined by the intramolecular hydrogen bond appear as a narrow band at  $3370\text{ cm}^{-1}$ , and asymmetric and symmetric  $\nu(CH)$  stretching vibrations of the methyl group appear as low-intensity absorption bands at  $3000$  and  $2970\text{--}2950\text{ cm}^{-1}$ . The bond vibrations  $\delta_{as}(NH)$ ,  $\nu_s(NCS)$ ,  $\delta(N-C-N)$ , and  $\nu(C=S)$  bonds are manifested in the frequency range from  $1700$  to  $800\text{ cm}^{-1}$ . The absorption bands at  $1600\text{--}1300\text{ cm}^{-1}$  are caused by vibrations of the benzamide group, those at  $1300\text{--}1000\text{ cm}^{-1}$  are due to vibrations of the thioureide fragment, and the bands at  $745\text{ cm}^{-1}$  are resulted from the C–H bending vibrations of the aromatic ring.

The absorption bands of functional groups of the ligand in the IR spectra of complexes **I**, **III**, and **IV** undergo the following shifts ( $\text{cm}^{-1}$ ):  $1605 \rightarrow 1585$  ( $\Delta\nu = 20$ ),  $1560 \rightarrow 1540$  ( $\Delta\nu = 20$ );  $1535 \rightarrow 1505$  ( $\Delta\nu = 30$ ),  $1490 \rightarrow 1520$  ( $\Delta\nu = 30$ );  $1350 \rightarrow 1372$  ( $\Delta\nu = 22$ );  $1280 \rightarrow 1225$  ( $\Delta\nu = 55$ );  $885 \rightarrow 917$  ( $\Delta\nu = 32$ ),  $815 \rightarrow 842$  ( $\Delta\nu = 27$ ). The  $\nu(OH)$  absorption band of the hydroxy group is absent from the spectra of complexes **I**, **II**, and **V** because of its deprotonation and formation of the M–O covalent bond. The  $\nu(OH)$  vibrations for complexes **III** and **IV** are observed at  $3400\text{ cm}^{-1}$ , which is associated with the monodentate coordination mode of the second thiosemicarbazide molecule. The low-frequency range of

**Table 2.** Binding energies for the main lines and components in the N1s, S2p<sub>3/2</sub>, Rh3d<sub>5/2</sub>, and Pd3d<sub>2/5</sub> spectra

Compound	N1s, eV	S2p, eV	Rh3d <sub>5/2</sub> , eV	Pd3d <sub>5/2</sub> , eV	Cl2p, eV
H <sub>4</sub> L	400.4 (400.1, 400.5, 401.2)	162.4			
<b>I</b>	400.7 (400.2, 400.7, 401.3)	163.7	310.6		198.2
<b>II</b>	400.9 (400.1, 400.8, 401.2)	163.6	310.3		
<b>III</b>	400.75 (400.1, 400.7, 401.2)	163.3		338.3	

these spectra exhibits an absorption band at 240–272 cm<sup>-1</sup> characteristic of stretching vibrations of the M ← S bond. The character of the IR spectra of complexes **III** and **IV** is identical, indicating in favor of the same coordination of the ligand to the central metal ion.

The intense broadened band at 1593 cm<sup>-1</sup> in the spectrum of complex **II** is caused by the superposition of several absorption bands corresponding to the vibrations of the C–C bond of the aromatic ring and ν(C=N) of the heterocycle. At the same time, the broad intense absorption band at 1100 cm<sup>-1</sup> caused by planar bending vibrations of the C–H bond of the aromatic ring is more pronounced compared to the corresponding absorption band at 1111 cm<sup>-1</sup> in the starting HBMHCTA, which is due to the conjugation of the phenol fragment with the triazole heterocycle. The ν(OH) absorption band is absent from the spectrum of complex **II** because of its deprotonation and formation of the Rh–O bond. In addition, the low-frequency range contains a new doublet band at 615 cm<sup>-1</sup> responsible for the transformation of C=S into (C–S)<sup>-</sup> [30], which is one of the key moments in the spectral characterization of complex **II**.

The XPS method makes it possible to determine both the valent state of the central atom and the nature of its donor environment. The values of binding energies of the internal electron levels (*E<sub>b</sub>*) of various platinum group metals allow one to determine the character of chemical bonds in coordination compounds with a high reliability [31, 32].

In rhodium complexes **I** and **II**, the values of *E<sub>b</sub>* Rh3d<sub>5/2</sub> are 310.6 and 310.25 eV, which corresponds to the trivalent state of the rhodium ion. The difference (Δ*E<sub>b</sub>* Rh3d<sub>5/2</sub> = 0.35 eV) in *E<sub>b</sub>* Rh3d<sub>5/2</sub> of the complexes is due to different characters of ligand coordination. It is known that the ligands having accepting groups of atoms (F, NO<sub>2</sub>, CO) withdraw the electron density from the central atom, thereby favoring an increase in *E<sub>b</sub>* of the metal.

Complexes **I** and **II** differ in both coordination and ligand nature. In complex **I**, the ligand contains the C=O accepting group, which can increase of the *E<sub>b</sub>* metal to 1 eV. However, this group does not participate in coordination, thus favoring an increase in Δ*E<sub>b</sub>*

Rh3d<sub>5/2</sub> by 0.35 eV only compared to that for compound **II**. Under the synthesis conditions of complex **II**, an alkaline medium results in ligand cyclization to form the triazole ring (scheme), due to which the carbonyl group is absent in complex **II**. For complexes **III** and **V**, *E<sub>b</sub>* Pd3d<sub>5/2</sub> = 338.15 and 338.05 eV, which completely corresponds to the divalent state of palladium ions.

The decomposition of the N1s spectral lines of thiosemicarbazide to components gave three values of *E<sub>b</sub>* N1s: 400.1, 400.6, and 401.2 eV corresponding to three nonequivalent states of the nitrogen atoms. The main N1s line consists of one band *E<sub>b</sub>* N1s = 400.4 eV corresponding to the protonated states of each nitrogen atom in the ligand molecule. In the case of formation of complex **I**, *E<sub>b</sub>* N1s of the main line remains unchanged, whereas in complex **II** *E<sub>b</sub>* N1s increases to 400.9 eV (Δ*E<sub>b</sub>* N1s = 0.5 eV). The value of one of the components also increases (Table 2), indicating in favor of the formation of the M ← N(L) coordination bond via the donor–acceptor mechanism. The nitrogen atom of the heterocycle participates in complex formation, and its donor–acceptor interaction with the metal results in an increase in *E<sub>b</sub>* N1s.

The decomposition of the N1s spectral line of complex **III** also gives three components of *E<sub>b</sub>* N1s: 400.1, 400.75, and 401.2 eV. The value of *E<sub>b</sub>* of the main N1s line increased to 400.75 eV, which is by 0.35 eV higher than that of uncoordinated thiosemicarbazide. This indicates in favor of Pd ← N(L) bond formation. It should be noted that the covalent radius of Pd<sup>2+</sup> is longer than that of Rh<sup>3+</sup>. This favors a stronger Pd–N interaction compared to Rh–N in complex **I** and, probably, results in an increase in *E<sub>b</sub>* N1s.

The energy characteristics of the S2p lines in the spectra of the initial ligand and complexes also differ. The shift of the S2p line of complexes **I–III** towards higher energies by 1.3–0.9 eV possibly indicates that the sulfur atom participates in coordination bonding. The increase in the S2p line in complex **II** by Δ*E<sub>b</sub>* S2p = 1.2 eV is due to the position of the sulfur atom near the system of conjugated bonds of the triazole ring with the aromatic ring.

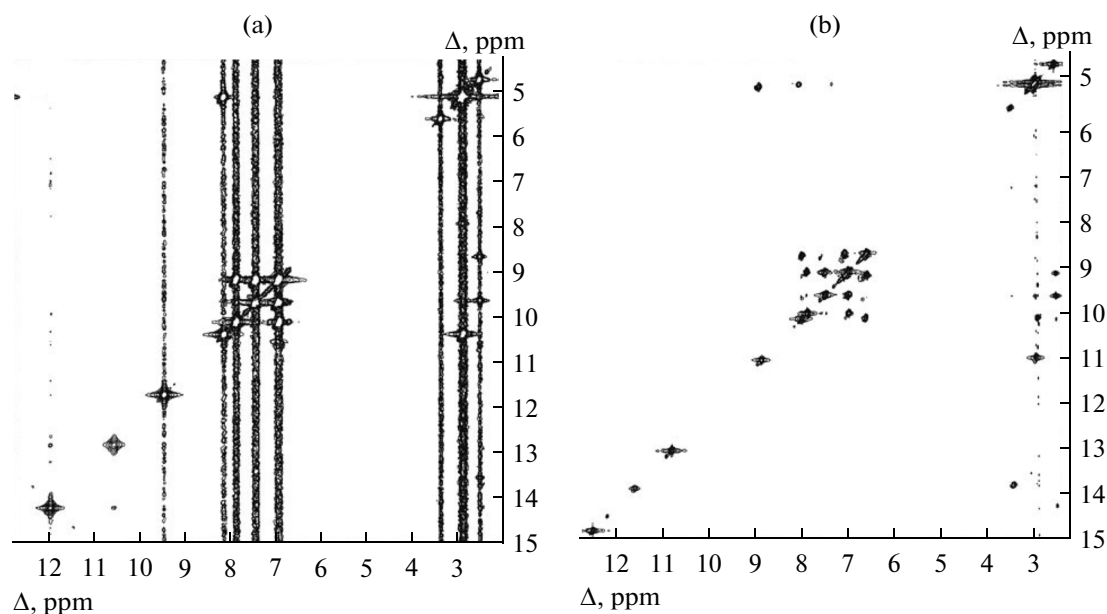


Fig. 3. COSY  $^1\text{H}$ – $^1\text{H}$  NMR spectra for (a) HBMHCTA and (b) complex **III**.

The value of  $E_b$  Cl $2p$  for complex **I** is 198.2 eV, which unambiguously indicates its out-of-sphere arrangement [31, 32]. No Cl $2p$  lines were detected for other complexes, indicating that complexes **II** and **III** contain no chlorine.

The  $^1\text{H}$  NMR spectrum of ligand  $\text{H}_4\text{L}$  exhibits a doublet signal from protons of the  $\text{CH}_3$  group with a chemical shift of 2.88 ppm. The range from 6.90 to 7.88 ppm contains signals from four protons of the benzene ring. The signal from the  $\text{N}^{(c)}\text{H}$  proton ( $\delta = 8.13$  ppm) was identified using nondiagonal cross-peaks in the 2D COSY  $^1\text{H}$ – $^1\text{H}$  NMR spectrum [33] (Fig. 3). Other low-field signals with  $\delta$  9.45, 10.55, and 11.95 ppm correspond to the  $\text{N}^{(a)}\text{H}$ ,  $\text{N}^{(b)}\text{H}$ , and OH protons, respectively [34, 35].

The  $^1\text{H}$  NMR spectrum of complex **I** exhibits a considerable downfield shift of all signals from the protons of the NH groups, which is caused by metal-cycle formation. The absence of the signal from the OH group in the spectrum indicates the deprotonation of this group and formation of the Rh–O bond. Unlike the spectrum of compound **I**, the low-field of the spectrum of complex **II** contains no signals from protons of all NH and CH groups, confirming the cyclization of thiosemicarbazide and thiazole ring formation in complex formation. To confirm the formation of the triazole ring, HBMHCTA cyclization was carried out under the conditions similar to those for the synthesis of complex **II**. The cyclization gave ligand  $\text{HL}'$ , whose  $^1\text{H}$  NMR spectrum is similar to that of complex **II**, except for the signal from the SH group, which is absent from the spectrum of the complex because of the formation of potassium salt. In addition, in the spectrum of complex **II**, the signals of the aromatic

ring undergo downfield shifts and no signal of the OH group is observed.

The  $^1\text{H}$  NMR spectra of complexes **III** and **IV** contain signals from two nonequivalent  $\text{CH}_3$  groups with  $\delta = 2.89, 2.94$  ppm in **III** and 2.90, 2.95 ppm in **IV**, as well as two sets of signals with the multiplicity characteristic of *ortho*-substituted benzene rings. The signals from the  $\text{N}^{(c)}\text{H}$  protons are at  $\delta = 7.92, 8.87$  ppm for **III** and 8.01, 8.80 ppm for **IV**. This double set of signals in the spectra of complexes **III** and **IV** indicates the mixed-type coordination of two ligand molecules to the central metal atom.

The  $^1\text{H}$  NMR spectrum of complex **V** consists of signals from the protons of triphenylphosphine in the coordination sphere of the complexes and from HBMHCTA, except for two singlets of the  $\text{N}^{(b)}\text{H}$  and OH groups.

A comparison of the  $^{13}\text{C}$  NMR spectra of complexes **III** and **IV** also indicates the identical coordination mode of the ligands in both compounds. As in the  $^1\text{H}$  NMR spectra, the doubled number of signals compared to the number of nonequivalent carbon atoms in the reactant molecule was observed, indicating the mixed-type coordination of two ligand molecules in each complex. For the carbon atom of the C=S group in HBMHCTA,  $\delta = 182.4$  ppm. This spectral range also exhibits signals at 178.2 and 168.4 ppm for **III** and at 176.8 and 167.9 ppm for **IV**. The values of  $\delta$   $^{13}\text{C}$  of one of sets of signals from the carbon atoms of the aromatic system differ insignificantly from the corresponding signals of  $\text{H}_4\text{L}$ , indicating the monodentate coordination of one of the ligand molecules [1]. On the contrary,  $\delta$  for the second set of signals for the corresponding carbon nuclei of the aromatic ring are

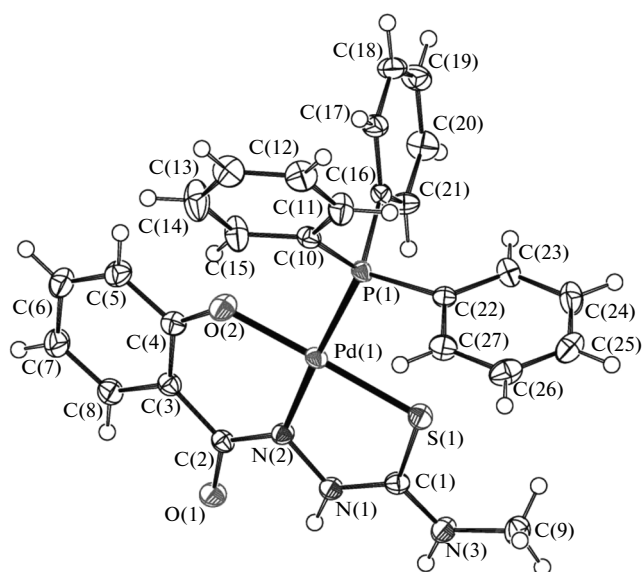


**Fig. 4.** Molecular structure of complex **V** (ellipsoids are presented with 50% probability).

noticeably shifted compared to the spectrum of  $H_4L$ , which confirms the coordination of the second ligand molecule through the chelate metalocycle. This coordination is also favored by a decrease in the intensity of the narrow  $\nu(OH)$  signals at  $3370\text{ cm}^{-1}$  in the IR spectra of complexes **III** and **IV**, which is a result of the participation of hydroxyl groups in the formation of intramolecular hydrogen bonds. Thus, the spectro-

**Table 3.** Bond lengths and bond angles in the structure of complex **V**

Bond	$d, \text{Å}$	Angle	$\omega, \text{deg}$
Pd(1)–N(2)	2.0099(17)	N(2)Pd(1)O(2)	90.72(6)
Pd(1)–O(2)	2.0143(16)	N(2)Pd(1)S(1)	86.04(5)
Pd(1)–S(1)	2.2612(6)	O(2)Pd(1)S(1)	176.15(5)
Pd(1)–P(1)	2.2698(5)	N(2)Pd(1)P(1)	175.90(5)
C(1)–S(1)	1.725(2)	O(2)Pd(1)P(1)	92.03(5)
C(2)–O(1)	1.265(2)	S(1)Pd(1)P(1)	91.098(19)
C(4)–O(2)	1.307(3)	N(1)C(1)N(3)	118.23(19)
C(1)–N(1)	1.322(3)	N(1)C(1)S(1)	120.17(16)
C(1)–N(3)	1.329(3)	N(3)C(1)S(1)	121.60(17)
N(1)–N(2)	1.397(2)	C(1)N(1)N(2)	120.33(17)
C(2)–N(2)	1.329(3)	C(2)N(2)N(1)	113.23(17)
		C(2)N(2)Pd(1)	131.38(14)
		N(1)N(2)Pd(1)	115.38(12)
		O(1)C(2)N(2)	120.40(19)
		O(1)C(2)C(3)	120.91(18)
		N(2)C(2)C(3)	118.65(18)

scopic studies confirm the structures of complexes **III** and **IV** shown in the scheme.

Complex **V** studied by X-ray diffraction analysis crystallizes with one ligand molecule in the symmetrically independent part (Fig. 4). The palladium atom forms a weakly distorted square environment with a molecule of ligand  $H_2L$  coordinated through the tridentate mode and supplemented by the triphenylphosphine molecule. The deviation from the root-mean-square plane of the Pd(1)O(2)N(2)S(1)P(1) coordination node is  $0.0153\text{ Å}$ . The Pd–O, Pd–N, Pd–S, and Pd–P bond lengths in complex **V** (Table 3) correspond to the published data for compounds of this type [36, 37].

The values of contiguous angles in the coordination environment of palladium range from  $86.04(5)^\circ$  to  $92.03(5)^\circ$  (Table 3), which can be due to the steric influence of the metalocycle and the bulky triphenylphosphine molecule. Molecule **V** includes two planar metalocycles Pd(1)O(2)C(4)C(3)C(2)N(2) (the deviation from the root-mean-square plane is  $0.0402\text{ Å}$ ) and Pd(1)N(2)N(1)C(1)S(1) (the deviation from the root-mean-square plane is  $0.0293\text{ Å}$ ) conjugated at the N(2) atom and forming a dihedral angle of  $6.45(7)^\circ$ . The  $H_2L$  molecule contains a conjugated system of double bonds, which are difficult to be localized on the basis of the geometric parameters. The C(1)–S(1), C(1)–N(1), C(1)–N(3) and C(2)–O(1), C(2)–N(2) bond lengths (Table 3) correspond to the published data for sesquialteral bonds between the corresponding atoms. In crystal structure **V**, the molecules are joined by the hydrogen bonds N(1)–H(1N)···O(1)<sup>#1</sup> (N···O  $2.824(2)\text{ Å}$ , angle NHO  $140(2)^\circ$ ) and N(3)–H(3N)···O(1)<sup>#1</sup> (N···O  $2.783(2)\text{ Å}$ , angle NHO  $153(2)^\circ$ ); <sup>#1</sup>  $-x + 2, -y, -z$  for the centrosymmetric dimers (Fig. 5).

Thus, we synthesized complexes **I–V**, whose molecular structures were determined from the data of elemental analyses and UV-VIS, IR, XPS, and  $^1\text{H}$  and  $^{13}\text{C}$  NMR spectroscopy. Rhodium cationic complex **I** with the tridentate-cyclic coordination of two molecules of the organic ligand and formation of the octahedral coordination node  $\text{RhS}_2\text{O}_2\text{N}_2$  was isolated from an acidic medium (pH 3) at the molar ratio  $M : L = 1 : 2$ .

In an alkaline medium (pH 9) at  $M : L = 1 : 2$ , HBMHCTA undergoes cyclization with triazole ring formation. The latter participates in coordination to the central metal ion, resulting in the formation of complex **II** and the six-membered metalocycle, as well as the octahedral node  $\text{RhO}_3\text{N}_3$ .

The coordination compounds of palladium (**III**) and platinum (**IV**) with the mixed-type (tridentate and monodentate) coordination modes of the ligand were isolated at pH 2 and reactant ratio  $M : L = 1 : 2$ . This specific feature of the coordination of HBMHCTA to the central metal ion appears in the  $^1\text{H}$  and  $^{13}\text{C}$  NMR spectra as a double set of all  $^1\text{H}$  and  $^{13}\text{C}$  signals.

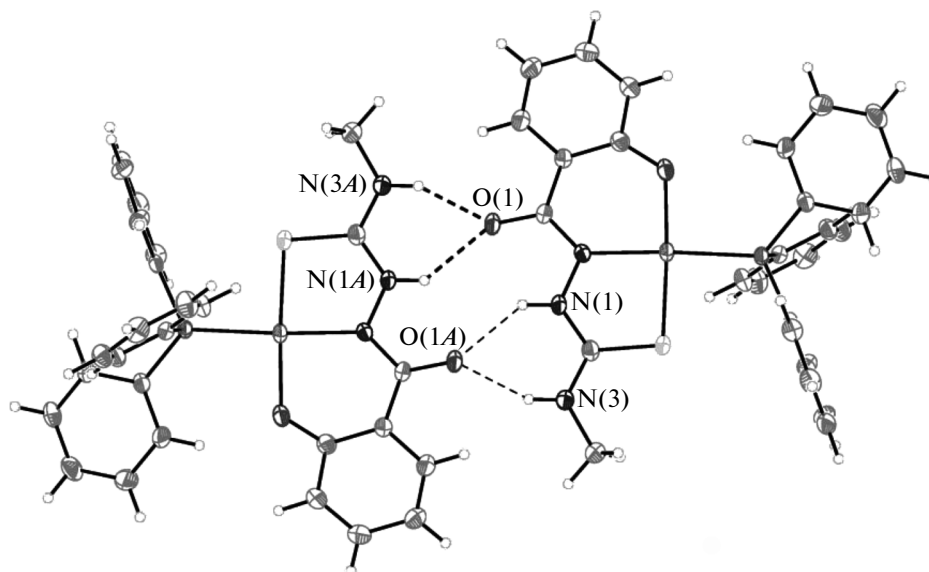


Fig. 5. Centrosymmetric dimers in crystal structure V (hydrogen bonds are designated by dashed lines).

The molecular structures proposed for complexes III and IV are indirectly confirmed by the result of the X-ray diffraction analysis of complex V in which the HBMHCTA molecule is coordinated according to the tridentate mode proposed for complexes III and IV.

#### REFERENCES

- Orysyk, S.I., Bon, V.V., and Zholob, O.O., et al., *Polyhedron*, 2013, vol. 51, p. 211.
- Orysyk, S.I., Bon, V.V., Pekhnyo, V.I., et al., *Polyhedron*, 2012, vol. 38, p. 15.
- Orysyk, S.I., Bon, V.V., Obolentseva, O.O., et al., *Inorg. Chim. Acta*, 2012, vol. 382, p. 127.
- Ali, M.A., Mirza, A.H., and Butcher, R.J., et al., *J. Inorg. Biochem.*, 2002, vol. 92, p. 141.
- Ablov, A.V., Bologa, O.A., and Samus', N.M., *Zh. Neorg. Khim.*, 1973, vol. 18, no. 1, p. 159.
- Rupesh, N.P. and Rengan, R., *Tetrahedron Lett.*, 2013, vol. 54, p. 1120.
- Yang, H., Chellan, P., Li, T., et al., *Tetrahedron Lett.*, 2013, vol. 54, p. 154.
- Kostas, I.D., Heropoulos, G.A., Kovala-Demertzi, D., et al., *Tetrahedron Lett.*, 2006, vol. 47, p. 4403.
- Prabhu, R.N. and Ramesh, R., *Tetrahedron Lett.*, 2012, vol. 53, p. 5961.
- Xie, G., Chellan, P., Mao, J., et al., *Adv. Synth. Catal.*, 2010, vol. 352, p. 1641.
- Garoufis, A., Hadjikakou, S.K., and Hadjiliadis, N., *Coord. Chem. Rev.*, 2009, vol. 253, p. 1384.
- Chellan, P., Shunmoogam-Gounden, N., and Hendricks, D.T., et al., *Eur. J. Inorg. Chem.*, 2010, vol. 2010, no. 22, p. 3528.
- Chellan, P., Nasser, S., Vivas, L., et al., *J. Organomet. Chem.*, 2010, vol. 695, p. 2225.
- Hernández, W., Paz, J., Vaisberg, A., et al., *Bioinorg. Chem. Appl.*, 2008, vol. 2008, doi: 10.1155/2008/690952
- Kovala-Demertzi, D., Millerb, J.R., Kourkoumelisa, N., et al., *Polyhedron*, 1999, vol. 18, p. 1005.
- Lederer, M., *An Introduction to Paper Electrophoresis*, Amsterdam: Elsevier, 1957.
- SHELXTL*, Madison (WI, USA): Bruker AXS Inc., 2001.
- Bon, V.V., Orysyk, S.I., Pekhnyo, V.I., and Volkov, S.V., *J. Mol. Struct.*, 2010, vol. 984, p. 15.
- Shaker, R.M., *Arkivoc*, 2006, vol. 2006, no. 9, p. 59.
- Sahni, S.K., Jain, P.C., and Rana, V.B., *Indian J. Chem., Sect. A: Inorg., Bio-inorg., Phys., Theor. Anal. Chem.*, 1979, vol. 18, p. 161.
- Afzaletdinova, N.G., Murinov, Yu.Sh., Vályamova, F.G., and Vasil'eva, E.V., *Russ. J. Inorg. Chem.*, 1999, vol. 44, no. 2, p. 183.
- Orysyk, S.I., Rybachuk, L.N., Pekhno, V.I., et al., *Russ. J. Inorg. Chem.*, 2010, vol. 55, no. 7, p. 1075.
- Lever, A.B.P., *Inorganic Electronic Spectroscopy*, Amsterdam: Elsevier, 1987, vol. 1.
- Singh, R.V., Fahmi, N., and Biyala, M.K., *J. Iranian Chem. Soc.*, 2005, vol. 2, no. 1, p. 40.
- Agarwal, R.K. and Prasad, S., *Turk. J. Chem.*, 2005, vol. 29, no. 3, p. 289.
- Kazitsyna, L.A. and Kupletskaya, N.B., *Primenenie UF-, IK- i YaMR-spektroskopii v organicheskoi khimii* (The Use of UV, IR, and BNR Spectroscopy in Organic Chemistry), Moscow: Vyssh. Shkola, 1971.
- Pekhnyo, V.I., Orysyk, S.I., Bon, V.V., and Orysyk, V.V., *Pol. J. Chem.*, 2006, vol. 80, p. 1767.
- Bon, V.V., Orysyk, S.I., Pekhnyo, V.I., et al., *Polyhedron*, 2007, vol. 26, p. 2935.

29. Orsyk, S.I., Rybachuk, L.N., Pekhn'o, V.I., and Orsyk, V.V., *Russ. J. Inorg. Chem.*, 2011, vol. 56, no. 11, p. 1747.
30. Pandey, O.P., Sengupta, S.K., Mishra, M.K., and Tripathi, C.M., *Bioinorg. Chem. Appl.*, 2003, vol. 1, no. 1, p. 35.
31. Nefedov, V.I., *Koord. Khim.*, 1975, vol. 1, no. 3, p. 291.
32. Nefedov, V.I., *Rentgenoelektronnaya spektroskopiya khimicheskikh soedinenii (X-ray Electron Spectroscopy of Chemical Compounds)*, Moscow: Khimiya, 1984.
33. Braun, S., Kalinowski, H.O., and Berger, S., *150 and More Basic NMR Experiments*, Wiley-VCH, 1998, p. 34.
34. Deromó, A.E., *Modern NMR Techniques for Chemistry Research*, Ustynyuk, Yu.A., Eds., Pergamon, 1987.
35. Volovenko, Yu.M. and Turov, O.V., *Yadernii magnitnii rezonans (Nuclear Magnetic Resonance)*, Kiev: Irpen': VTF Perun, 2007.
36. Adoracion, G.Q., Cubo, E., Blas, E., et al., *J. Inorg. Biochem.*, 2007, vol. 101, p. 104.
37. Allen, F.H., Kennard, O., Watson, D.G., et al., *J. Chem. Soc., Perkin Trans.*, 1987, no. 2, p. S1.

*Translated by E. Yablonskaya*